JPE 15-5-2

http://dx.doi.org/10.6113/JPE.2015.15.5.1158
ISSN(Print): 1598-2092 / ISSN(Online): 2093-4718

A Hybrid PWM-Resonant DC-DC Converter for Electric Vehicle Battery Charger Applications

Il-Oun Lee†

†Department of Electrical Energy Engineering, Keimyung University, Daegu, Korea

Abstract

In this paper, a new hybrid DC-DC converter is proposed for electric vehicle 3.3 kW on-board battery charger applications, which can be modulated in a phase-shift manner under a fixed frequency or frequency variation. By integrating a half-bridge (HB) LLC series resonant converter (SRC) into the conventional phase-shift full-bridge (PSFB) converter with a full-bridge rectifier, the proposed converter has many advantages such as a full soft-switching range without duty-cycle loss, zero-current-switching operation of the rectifier diodes, minimized circulating current, reduced filter inductor size, and better utilization of transformers than other hybrid dc-dc converters. The feasibility of the proposed converter has been verified by experimental results under an output voltage range of 250-420V dc at 3.3 kW.

Key words: Battery charger, Electric vehicle, Phase-shift full-bridge converter

I. INTRODUCTION

For electric vehicle (EV) applications, an AC-DC converter is required for use as a battery charger. In general, the battery charger for EVs consists of a power factor corrector and an isolated DC-DC converter that directly recharges the battery in EVs [1]-[5]. During the battery recharging process, the output of the DC- DC converter varies greatly within a specific voltage range and its operating range becomes very wide. This makes it difficult to optimally design a converter in the sense of power conversion efficiency.

A conventional phase-shift full-bridge (PSFB) converter with a full-bridge rectifier is the preferred DC-DC topology for EV on-board battery charger applications, because of its natural zero-voltage-switching (ZVS) operation, low current ripple in the battery charging current, and simple structure and control [6]-[8]. However, for wide-output-voltage-range applications like battery chargers, the conventional PSFB converter cannot obtain an optimal power conversion efficiency due to its unique drawbacks such as a narrow ZVS range, large circulating current, and high voltage stress in the rectifier diodes [9]-[11]. In order to improve the performance of the conventional PSFB converter for EV battery charger applications, hybrid dc-dc converters with an LLC series resonant converter (SRC) integrated into the PSFB converter have recently been researched [12]-[14]. By integrating an LLC SRC into a PSFB converter, the resulting hybrid dc-dc converters have many advantages such as a wide ZVS range, reduced size of the filter inductor, and reduced voltage stress. Furthermore, the hybrid converter can work with a reduced operating range during the battery recharging process. Thus, it is possible to obtain a more optimal power conversion efficiency.

This paper proposes a novel hybrid PWM-resonant converter with a half-bridge (HB) LLC SRC integrated into a conventional PSFB converter with a full-bridge rectifier (FBR). While the proposed converter has all of the benefit of the hybrid converters in [12]-[14], it has fewer components and better utilization of the transformers when compared with previous hybrid converters. The circuit configuration, operating principle, and analysis of the proposed converter are presented in this paper. Its feasibility is verified with experimental results under an output voltage range of 250-420 V dc at 3.3 kW.

II. DESCRIPTION OF THE PROPOSED CONVERTER

A circuit diagram of the proposed converter is shown in Fig. 1. As can be seen, it is based on a conventional PSFB converter with a FBR. In addition, a half-bridge (HB) LLC

Manuscript received Jan. 2, 2015; accepted Mar. 16, 2015
Recommended for publication by Associate Editor Bor-Ren Lin.
†Corresponding Author: leeiloun@kmu.ac.kr
Tel: +82-53-580-5252, Fax: +82-53-580-5165, Keimyung University
Dept. of Electrical Energy Eng., Keimyung University, Korea

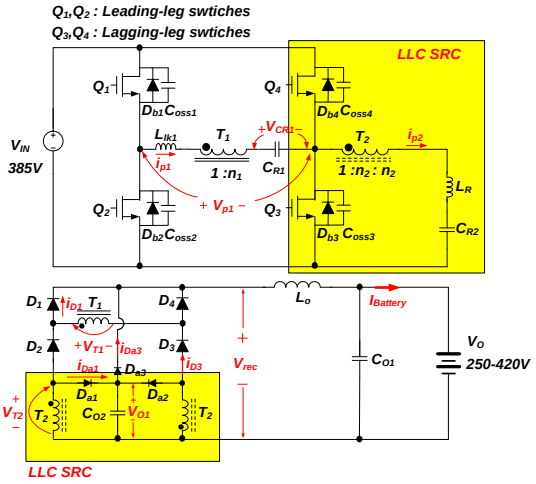

Fig. 1. Proposed converter for electric vehicle on-board battery charger applications.

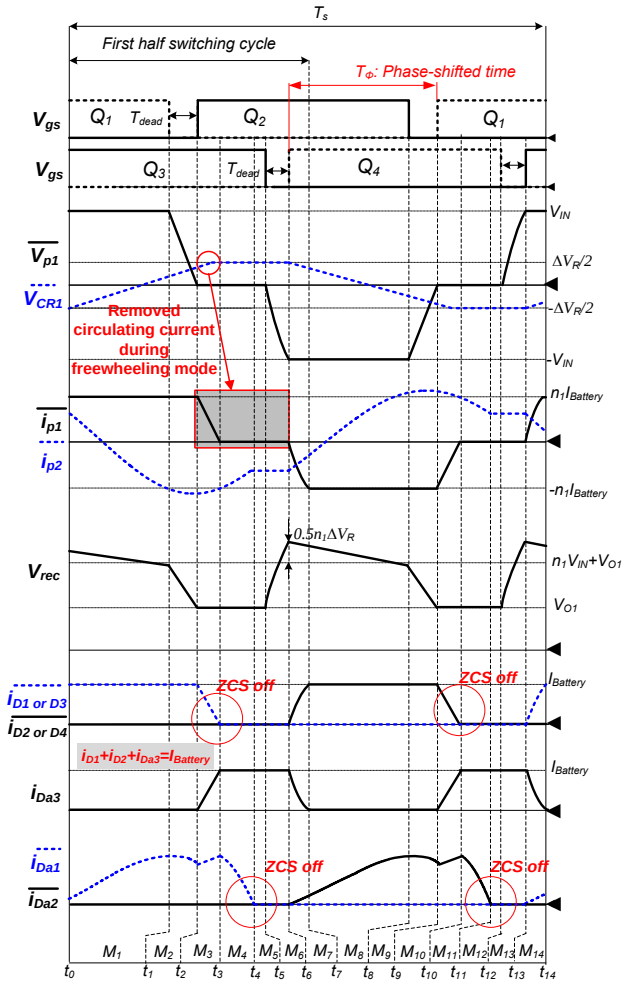

Fig. 2. Key waveforms of the proposed converter.

SRC with a center-tap rectifier (CTR) is integrated into the conventional converter by sharing the lagging-leg switches Q_3 and Q_4 and stacking two rectifiers in series before the output filter stage consisting of L_O and C_{O1}. The lagging-leg switches in the conventional PSFB converter fail easily in terms of ZVS operation as the output load decreases [6]-[8]. However, the lagging-leg switches in the proposed converter can achieve ZVS operation without the effect of the output load condition due to the integrated LLC SRC as documented in [12]-[14]. Moreover, the circulating current flowing only in the primary side of the conventional PSFB converter is removed because the primary current is reset to zero level with the voltage ripple of the resonant capacitor C_{R1} during the freewheeling phase, as shown in the key operating waveforms of the proposed converter described in Fig. 2. In the process, the rectifier diodes $D_{1\text{-}4}$ can be turned off with the zero-current-switching (ZCS) operation. The other output diodes Da_1 and Da_2 are also turned off with the ZCS due to the resonant operation of the LLC SRC. With these improvements, the proposed converter can achieve a higher power conversion efficiency when compared to the conventional PSFB converter. In addition, it can maintain a high efficiency during the battery recharging process.

A. Operation Principle

In order to analyze the operation of the proposed converter, several assumptions are made as follows.

1) The switch devices are ideal MOSFETs except for the parasitic capacitors and the internal body diodes;
2) The parasitic capacitors of all the MOSFETs have the same capacitance as C_{OSS};
3) The rectifier diodes are ideal;
4) The output inductor L_O is large enough to be treated as a constant current source during a switching period;
5) The magnetizing inductance of T_1 is very large so that the magnetizing current can be ignored;
6) The leakage inductor of T_2 is included into the resonant inductor L_R;

The driving signals are the same as those for the conventional PSFB converter and the output is regulated in the phase-shift manner at a fixed frequency, which is also the same as the conventional converter. Referring to Fig. 2, there are 14 operating modes in a switching period which can be divided into two half cycles: t_0-t_7 (from mode 1 to mode 7) and t_7-t_{14} (from mode 8 to mode 14). The operation principles of two half cycles are symmetric. Therefore, only the first half cycle is described and operating circuits during the cycle are shown in Fig. 3.

Mode 1 [t_0-t_1]: Mode 1 begins when the switches Q_1 and Q_3 are in the ON-state, and it ends when the switch Q_1 is turned off. The output current $I_{Battery}$ flows through the diodes $D_{1\&3}$ and the transformers of T_1 and T_2. The capacitor C_{O2} is charged with the resonant current generated by the resonance between L_R and C_{R2} in the LLC SRC via the diode D_{a2}. During this mode, the voltage across the resonant capacitor C_{R1} is linearly charged by the load current (or $n_1 I_{Battery}$) reflected to the primary side and it can be expressed as:

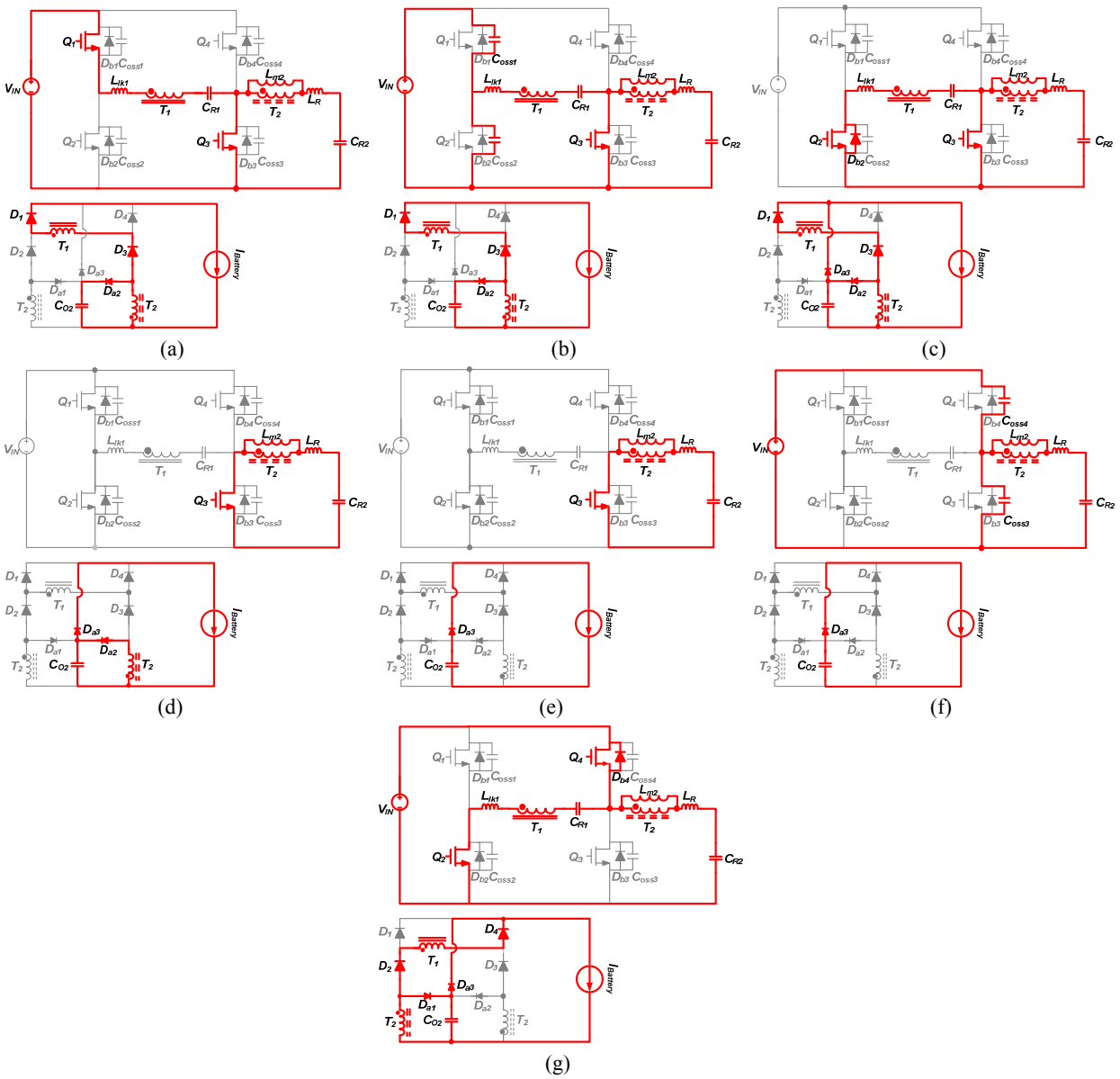

Fig. 3. Operating circuits of the proposed converter. (a) Mode 1. (b) Mode 2. (c) Mode 3. (d) Mode 4. (e) Mode 5. (f) Mode 6. (g) Mode 7.

$$V_{CR1}(t)=\frac{n_1 I_{Battery}}{C_{R1}}(t-t_0)-0.5\Delta V_R,$$

where $\Delta V_R \approx \frac{n_1 D I_{Battery} T_S}{C_{R1}}$. (1)

The rectifier output voltage $V_{rec}(t)$ is the sum of the voltages of the transformers and it is expressed as:

$$V_{rec}(t)=V_{T1}(t)+V_{T2}(t)=n_1(V_{IN}-V_{CR1}(t))+V_{O1}. \quad (2)$$

From eq. (2), it is known that both the PSFB and LLC converters transfer the power required in the output port.

Mode 2 [t_1-t_2]: Mode 2 begins when the switch Q_1 is turned off and it ends when the primary voltage $V_{P1}(t)$ reaches the zero level. Since the output current $I_{Battery}$ still flows through $D_{1\&3}$, the voltages across Q_1 and Q_2 are linearly charged or discharged by the energy stored in the output inductor L_O as follows:

$$V_{Q1}(t)=\frac{n_1 I_{Battery}}{2C_{OSS}}(t-t_1) \text{ and } V_{Q2}(t)=V_{IN}-V_{Q1}(t)=V_{P1}(t). \quad (3)$$

$V_{P1}(t)$ decreases linearly to the zero level as $V_{Q2}(t)$ and $V_{rec}(t)$ also ramps down to the output of the LLC SRC, V_{O1}. The equation for $V_{rec}(t)$ is the same as Equation (2). The resonant current of the LLC SRC continuously charges C_{O1}.

At the end of this mode, the switch Q_2 is turned on with ZVS.

Mode 3 [t_2-t_3]: Mode 3 begins when the switch Q_2 is turned on with ZVS, and it ends when the primary current $i_{P1}(t)$ reaches the zero level. During this mode, $V_{P1}(t)$ is zero, $i_{P1}(t)$ is reset to the zero level with the voltage ripple of C_{R1} as in eq. (4), and commutation occurs between the output diodes $D_{1\&3}$ and D_{a3}.

$$i_{P1}(t) = n_1 I_{Battery} - \frac{0.5\Delta V_R}{L_{lk1}}(t - t_2). \quad (4)$$

$V_{rec}(t)$ is the output of the LLC SRC, V_{O1}. This means that only the LLC SRC transfers the power required in the output port.

In this mode, the circulating current existing in the conventional PSFB converter is removed, and the output diodes $D_{1\&3}$ are turned off with ZCS. Consequently, the conduction power loss in the active switches and the switching power loss in the rectifier diodes are reduced during the battery recharging process.

Mode 4 [t_3-t_4]: Mode 4 begins when the commutation between $D_{1\&3}$ and D_{a3} is completed, and it ends when the power transfer by the LLC SRC (from V_{IN} to C_{O1}) is completed. In this mode, the output power is supplied from the output of the LLC SRC as in Mode 3. At the end of this, the diode D_{a2} is turned off with ZCS.

Mode 5 [t_4-t_5]: Mode 5 begins when the power transfer by the LLC SRC is completed, and it ends when the switch Q_3 is turned off. The output power is supplied from the output of the LLC SRC as always. The primary current $i_{P2}(t)$ becomes the magnetizing current of the transformer T_2 in this mode.

Mode 6 [t_5-t_6]: Mode 6 begins when Q_3 is turned off, and it ends when $V_{P1}(t)$ reaches -V_{IN}. During this mode, the voltages across Q_3 and Q_4 are charged or discharged by the energy stored in the magnetizing inductor L_{m2} of T_2 as follows:

$$V_{Q3}(t) = \frac{i_{P2}(t_5)}{2C_{OSS}}(t - t_5) = \frac{i_{Lm2}(t_5)}{2C_{OSS}}(t - t_5) \quad \text{and}$$
$$V_{Q4}(t) = V_{IN} - V_{Q3}(t). \quad (5)$$

At the end of this mode, the switch Q4 is turned on with ZVS.

Mode 7 [t_6-t_7]: Mode 7 begins when the switch Q_4 is turned on with ZVS. Since $V_{P1}(t)$ is the negative input voltage, $i_{P1}(t)$ is decreased as in eq. (6) and the commutation between the output diodes $D_{2\&4}$ and D_{a3} occurs. The resonance between L_R and C_{R2} is progressed in the LLC SRC and the resonant current generated by the resonance starts to flow to C_{O1} via D_{a1}.

$$i_{P1}(t) = -\frac{V_{IN} - 0.5\Delta V_R}{L_{lk1}}(t - t_6). \quad (6)$$

The rectifier output voltage $V_{rec}(t)$ is equal to eq. (2), and both the PSFB and LLC converters start to transfer the power required in the output port. This mode ends when the commutation between $D_{2\&4}$ and D_{a3} is completed.

B. Voltage Conversion Ratio, M

The $V_{rec}(t)$ in Fig. 2 can be simplified as in Fig. 4(a) after ignoring the durations of modes 2 and 6 because their durations are very narrow in practice. Fig. 4(b) shows $V_{rec}(t)$ in the conventional PSFB converter with a FBR. As shown in the figure, the conventional PSFB converter processes only the power transfer within the powering interval defined as the

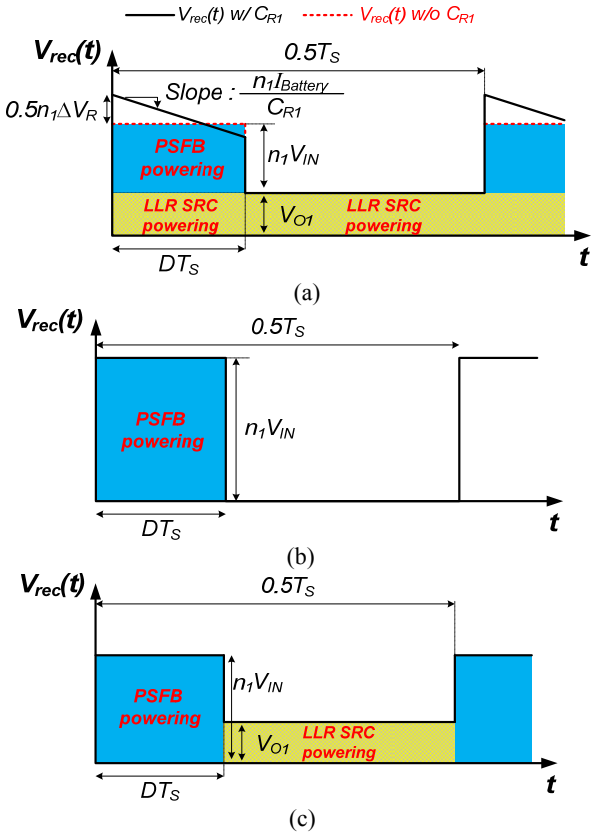

Fig. 4. Output voltage waveform of rectifier: (a) in the proposed converter, (b) in the conventional PSFB converter, and (c) in the hybrid converters in [12] and [13].

effective duty-cycle time, DT_S. On the other hand, the proposed converter continuously transfers the power required in the output port with the help of the LLC SRC. Due to the difference between these powering concepts, the proposed converter can have a lower turns-ratio of T_1 when compared with the conventional PSFB converter as in eq. (7).

$$n_{1\_proposed\_converter} << n_{1\_conventional\_converter}. \quad (7)$$

Since the lower turns-ratio reduces both the conduction power loss generated in the primary side of the transformers and the voltage stress in the rectifier diodes, it is possible that the proposed converter gets a power conversion efficiency that is better than the conventional PSFB converter for charging the battery.

Since the voltage across C_{R1} in the proposed converter is small in practice, consider the $V_{rec}(t)$ without the effect of C_{R1} in Fig. 4(a) for getting the voltage conversion ratio of the proposed converter. The voltage conversion ratio, M can be obtained by averaging $V_{rec}(t)$ as:

$$M(D) = \frac{V_O}{V_{IN}} = 2n_1 D + 0.5 n_2 M_{LLC\_SRC}, \quad (8)$$

where D is the duty-cycle that is a function of the phase-shifted time, T_ϕ as $D = T_\phi / T_S$.

In eq. (8), M_{LLC_SRC} is the gain of the LLC SRC and is defined as:

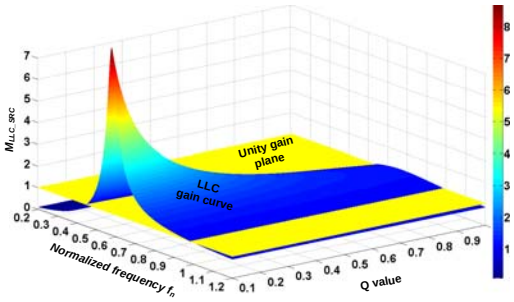

Fig. 5. Gain (M_{LLC_SRC}) curve of LLC SRC [16].

$$M_{LLC\_SRC}=\frac{V_{O1}}{n_2(V_{IN}/2)}=\frac{k}{\sqrt{\left(1+k-\frac{1}{f_n^2}\right)^2+Q^2k^2\left(f_n-\frac{1}{f_n}\right)^2}}, \tag{9}$$

where:

$$Q=\frac{1}{R_{ac}}\sqrt{\frac{L_R}{C_{R2}}},\quad k=\frac{L_{m2}}{L_R},\quad f_R=\frac{1}{2\pi\sqrt{L_RC_{R2}}},\quad f_n=\frac{f_S}{f_R},$$

$R_{ac}=\frac{8R_L}{(n_2\pi)^2}$, $R_L=V_{O1}/I_{battery}$, and f_S is the switching frequency.

From eq. (8), it is known that the output of the proposed converter can be regulated with three methods: phase-shift modulation at a fixed frequency, frequency modulation at a fixed duty-cycle, and hybrid modulation of the duty-cycle and frequency. In this paper, the control is focused on only the phase-shift modulation at a fixed frequency, which is the same as the conventional PSFB converter.

Fig. 5 shows the curve of M_{LLC_SRC}. If the resonant frequency of the LLC SRC, f_R is designed with the same magnitude as the switching frequency, M_{LLC_SRC} has a gain value of 1.0 as shown in the figure. Then, eq. (8) can be fruther simplified and M can be expressed by normalizing the voltage conversion ratio based on the turns-ratio n_1 of the PSFB transformer as:

$$M_{norm\_proposed}(D)=\frac{V_O}{n_1V_{IN}}=2D+0.5\alpha, \tag{10}$$

where $0<\alpha(=n_2/n_1)\le 1$.

Fig. 6 shows the curve of eq. (10). As can be seen, the gain of the proposed converter is always larger than that of the conventional PSFB converter. From this, it is known once more that the turns-ratio of T_1 in the proposed converter can be designed with a smaller value when compared with the conventional converter as in eq. (7).

C. Transformer Utilization, T.U

Fig. 4(c) shows the $V_{rec}(t)$ of the hybrid converters in [12] and [13]. As can be seen in the figure, the powering sections of the PSFB converter and the LLC SRC are separated over a switching period. This scheme lowers the utilization of the

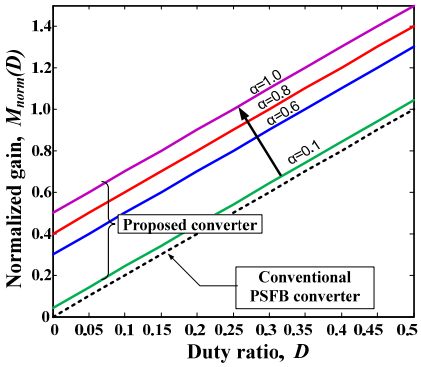

Fig. 6. Voltage conversion ratio of proposed converter when f_R=f_S.

transformers for the battery charger applications as mentioned in [15]. For example, if the converters charge a battery with the CC-CV charging strategy, the *T.U* in the converters can be calculated as follows:

$$\begin{aligned}T.U&=\frac{P_{out(\max)}}{P_{PSFB(\max)}+P_{LLC\_SRC(\max)}}\\&=\frac{V_{O(\max)}\cdot I_{Battery}}{V_{O(\max)}\cdot I_{Battery}+V_{O(\min)}\cdot I_{Battery}}\\&=\frac{420[V]\bullet I_{Battery}}{420[V]\bullet I_{Battery}+250[V]\bullet I_{Battery}}=0.67.\end{aligned} \tag{11}$$

On the other hand, the PSFB converter in the proposed converter always receives the help of the LLC SRC in processing the power transfer. In this structure, the *T.U* is calculated as follows:

$$\begin{aligned}T.U&=\frac{V_{O(\max)}\bullet I_{Battery}}{(V_{O(\max)}-V_{O1})\bullet I_{Battery}+V_{O1}\bullet I_{Battery}}=1.0\\&=\frac{420[V]\bullet I_{Battery}}{220[V]\bullet I_{Battery}+200[V]\bullet I_{Battery}}=1.0.\end{aligned} \tag{12}$$

Consequently, the proposed converter has better utilization of the transformers when compared with the hybrid converters in [12] and [13].

D. Reduction of the Circulating Current

The conventional PSFB converter working in the phase-shift manner has freewheeling phases. During the freewheeling phases, the non-powering current circulates in the primary side of the transformer. This current is officially called the circulating current, and it is pinpointed as a significant drawback of the conventional PSFB converter operating under wide output voltage range applications like battery chargers. This is because the freewheeling phases are maximized when the battery voltage is at its minimum value, and then the conduction power loss coming from the circulating current is maximized.

On the other hand, the circulating current is minimized in the proposed converter due to the voltage ripple of C_{R1} as analyzed in detail in mode 3. Aa a result, the RMS value of the primary current can be reduced and the conduction power

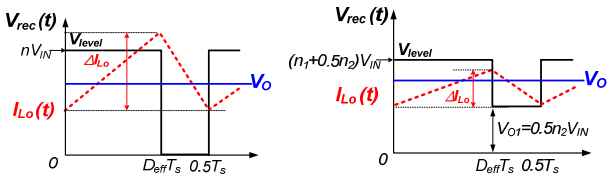

(a) (b)

Fig. 7. Current ripple of output inductor current. (a) Conventional PSFB converter. (b) Proposed converter.

loss can be also reduced.

E. Soft-Switching Characteristics

In the conventional PSFB converter, the ZVS operation of the leading-leg switches is less sensitive to output load conditions due to the large ZVS energy coming from the large output filter inductor. On the other hand, the lagging-leg switches fail very easily in terms of the ZVS operation as the output load current decreases. This is because the source of the ZVS energy is the energy stored in the small leakage inductor of T_1 and this energy is very small.

The ZVS operation of the leading-leg switches in the proposed converter is obtained with the same principle as the conventional PSFB converter. Hence, it is less sensitive to the output load condition. Meanwhile, the ZVS of the lagging-leg switches (or Q_3 and Q_4) is achieved with the energy stored in the magnetizing inductor of T_2 as explained in eq. (5). This is the same ZVS principle as LLC SRC. Therefore, the lagging-leg switches are always able to operate with ZVS without the effect of the output load.

All of the rectifier diodes in the conventional PSFB converter are under hard switching status. Meanwhile, for the proposed converter, the diodes D_1 and D_2 are turned off with ZCS due to the voltage ripple of C_{R1} as explained in mode 3. The diodes D_{a1} and D_{a2} are also turned off with ZCS due to the resonant process of the LLC SRC.

F. Duty-Cycle Loss

For a wide ZVS range, the conventional PSFB converter requires the addition of an external inductor. However, this method greatly increases the commutation time of the primary current and a very large duty-cycle loss occurs. To compensate for the increased duty-cycle loss, the turns-ratio of the transformer (*n*) should be designed with a larger value. As a result, both the current stress in the primary side of the transformer and the voltage stress of the rectifier diodes increase significantly.

Meanwhile, the ZVS range in the proposed converter is extended without adding an external inductor. As a result, the commutation time of the primary current is minimized, and the effective duty-cycle D_{eff} comes close to the real duty-cycle D, which is defined as $D = T_{\phi} / T_S$. Consequently, the turns-ratio of the PSFB transformer T_1 can be designed to be more beneficial when compared with the conventional PSFB converter.

TABLE I
COMPONENTS LIST

Main switches (Q_1~Q_4)	IPP60R074C6(650V)
Rectifier diodes (D_1,D_4)	F08H60S
Rectifier diodes (D_2,D_3)	IDH15S120
Rectifier diodes (D_{a1}~D_{a3})	10ETF04
Transformers (T_1)	Core – PQ5050, Turns-ratio (n_1) – 0.71 L_m - 1.0mH, L_{lk} -9.6μH
Transformers (T_2)	Core – PQ3535, Turns-ratio (n_2) – 1 L_m - 120μH, L_{lk} -7.3μH
Resonant inductor (L_R)	12.65μH
Resonant capacitor (C_{R1})	0.1μF/50V
Resonant capacitor (C_{R2})	0.1μF/1kV
Output inductor (L_O)	250μH (MPP core)
Output capacitor (C_{O1})	100μF/450V
Output capacitor (C_{O2})	4.7μF250V
Controller	TMS320F28069

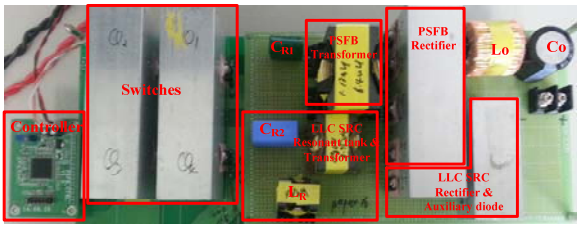

Fig. 8. Prototype board for the experiment of the proposed converter.

G. Filter Requirements

In the proposed converter, the output power is supplied continuously from the input stage over a switching period. Meanwhile, the conventional PSFB converter processes only the required power within the effective duty-cycle time due to the freewheeling phases. As a result of this difference, the proposed converter can have a much lower V_{level} and a smaller current ripple of the output inductor ΔI_{Lo} than the conventional converter, as shown in Fig. 7. In other words, the output inductor in the proposed converter can be designed with a much smaller inductance when compared with the conventional converter under the same specifications for the current ripple. Eq. (13) shows how to select a magnetic core for the design of the output inductor. As in the equation, the proposed converter can employ an output inductor with a smaller size due to the smaller inductance.

$$A_P > \frac{L \cdot I_{Lo}^2}{k_w \cdot \Delta B \cdot J}. \tag{13}$$

where A_P is the window-area product of the magnetic core, L is the required inductance, I_{Lo} is the RMS or DC value of the current flowing through the inductor, ΔB is the working flux density, J is the current density, and k_w is the winding factor.

III. EXPERIMENTAL RESULTS

To verify the effectiveness of the proposed converter, a 3.3 kW prototype circuit has been built with the components listed in Table I and tested with the battery charging strategy

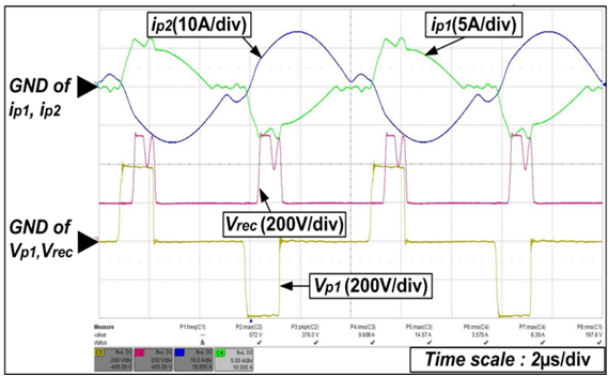

(a)

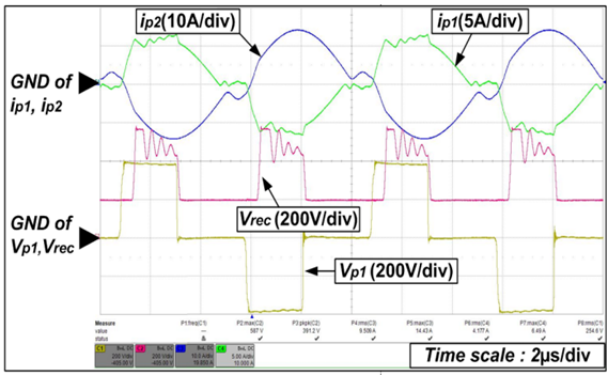

(b)

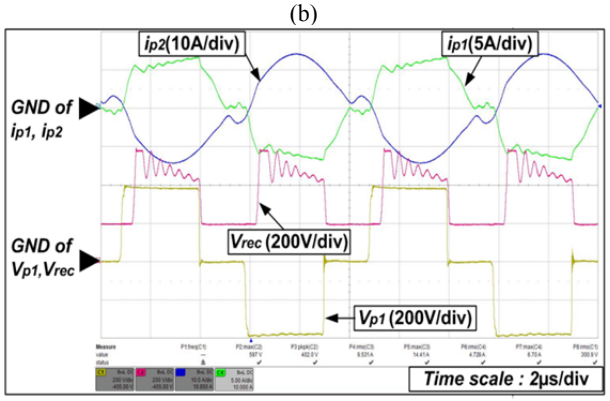

(c)

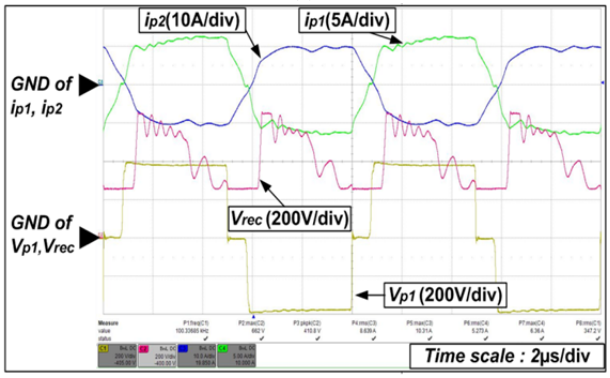

(d)

Fig. 9. Operating waveforms ($i_{p1}(t)$, $i_{p2}(t)$, $V_{p1}(t)$ and $V_{rec}(t)$) of the proposed converter during constant-current mode with the charging current of 7.85A: (a) when V_O=250V, (b) when V_O=300V, (c) when V_O=350V, and (d) when V_O=420V (100% load condition).

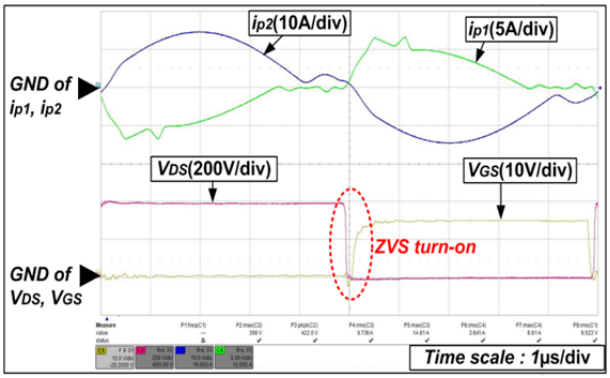

(a)

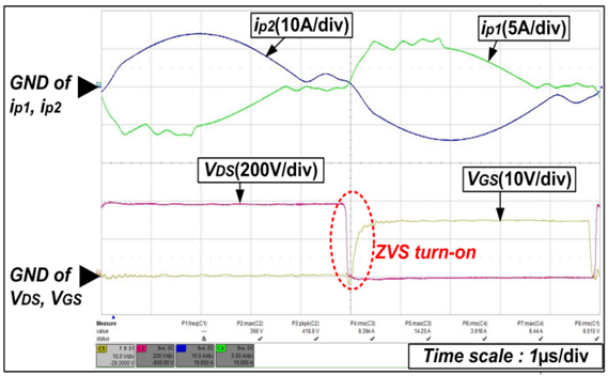

(b)

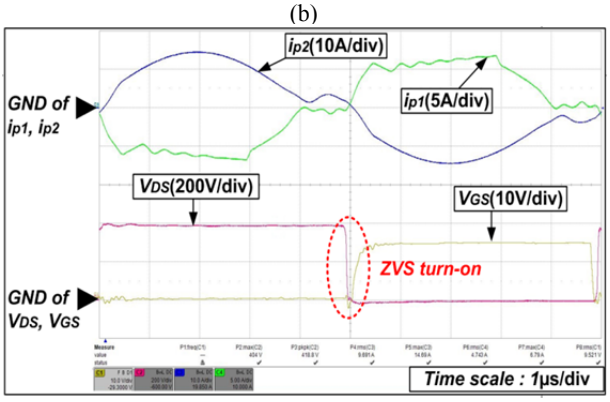

(c)

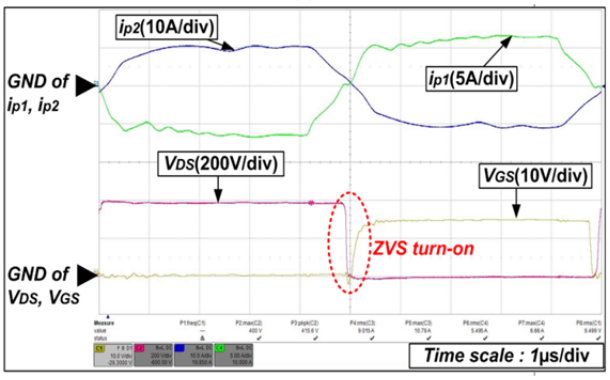

(d)

Fig. 10. ZVS waveforms of lagging-leg switches during constant-current mode with the charging current of 7.85A: (a) when V_O=250V, (b) when V_O=300V, (c) when V_O=350V, and (d) when V_O=420V (100% load condition).

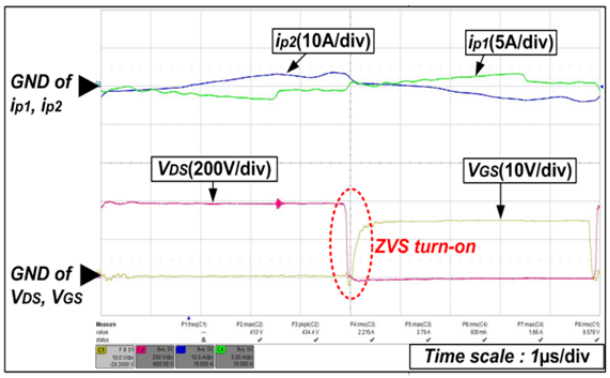

(a)

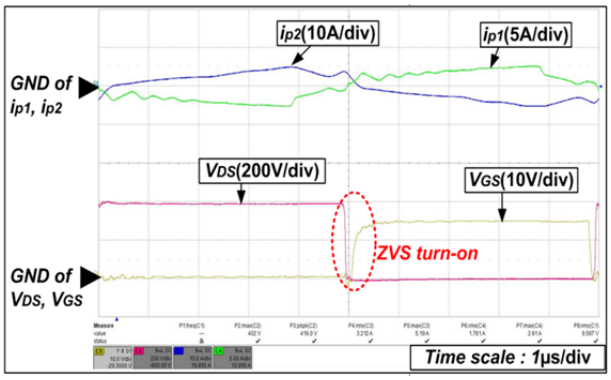

(b)

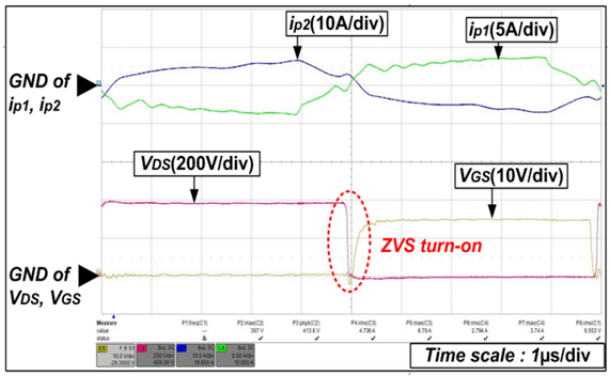

(c)

Fig. 11. ZVS waveforms of lagging-leg switches during constant-voltage mode at 420V: (a) when I_O=0.78A(10% load), (b) when I_O=1.57A(20% load), and (c) when I_O=3.93A(50% load).

consisting of the constant-current and constant voltage modes. Fig. 8 shows the prototype converter. The prototype circuit has the following specifications:

- Input voltage: V_{IN}=385 V
- Output voltage: V_O=250-420 V
- Charging curent during CC mode: $I_{Battery}$=7.85 A
- Switching frequency: f_S=100 kHz

The resonant tank of LLC SRC was designed with the following procedure. Firstly, in order to guarantee the ZVS operation of the lagging-leg switches, the following equation should be satisfied.

$$\frac{1}{2}L_{m2}i_{p2}^2(t_5) \geq \frac{1}{2}C_{OSS}V_{IN}^2 \quad \text{where} \quad i_{p2}(t_5) = \frac{V_{O1}}{4n_2 f_S L_{m2}}. \tag{13}$$

Eq. (13) can be represented as follows:

$$L_m \leq \frac{1}{C_{OSS}}\left(\frac{V_{O1}}{4n_2 f_S V_{IN}}\right)^2. \tag{14}$$

Considering the power handing capacity of the half-bridge LLC SRC in EV battery charger applications, the output voltage of the LLC SRC, V_{O1} was set as 200V. In order to minimize the circulating current generated by the LLC SRC, the resonant frequency (f_R) was designed with the same magnitude as the switching frequency (f_S). For the LLC SRC, the resonant frequency is the load-independent frequency to guarantee the ZVS turn on of the lagging-leg switches from zero to full load. In addition, the gain of the LLC SRC becomes 1.0 at this frequency. Then, in turn, from eq. (9), it can be noted that n_2 is equal to 1.0. According to equation (14), with the design parameters of n_2=1.0, V_{IN}=385V, V_{O1}=200V, C_{oss} of IPP60R074C6, and f_S=100 kHz, the magnetizing inductance of T_2, L_{m2} was designed as 120μH. In designing the LLC SRC, k is commonly designed in the range from 4.0 to 6.0 considering the input voltage variation and the conduction power loss. In this paper, k was selected as 6.0. Then, the resonant inductance for L_R is given as 20μH. Finally, the resonant capacitor C_{R2} can be designed with the following equation:

$$C_{R2} = \frac{1}{(2\pi f_R)^2 L_R} = 100nF. \tag{15}$$

For the control of the battery charging based on the CC-CV charging strategy, two control loops were used: an inner current control loop and an outer voltage control loop. In addition, two PI-type controllers were used to regulate the battery voltage and the charging current. The entire control diagram was digitally implemented using a TMS320F28069.

Fig. 9 shows the key operating waveforms of the proposed converter, while the battery is being charged from 250V to 420V with a constant-current of 7.85A. As shown in the figure, all of the measured waveforms follow the theoretical waveforms described in Fig. 2 well. Moreover, it is confirmed that the proposed converter has reduced the circulating current in the primary side when the primary voltage $V_{P1}(t)$ is at the zero level during the battery charging process. It can also be seen that there is a staircase voltage waveform in the output of rectifier, V_{rec} in the figure. From this, it is known that the output power is transferred continuously from the input stage to the output stage, and that the size of the output filter inductor can be smaller than that of the conventional PSFB converter.

Figs. 10 and 11 show the ZVS waveforms of the lagging-leg switches during the battery charging process. As can be seen, the lagging-leg switches are successfully turned on with ZVS under the overall load conditions due to the combination with an LLC resonant converter.

Fig. 12 shows the efficiency measured during the battery

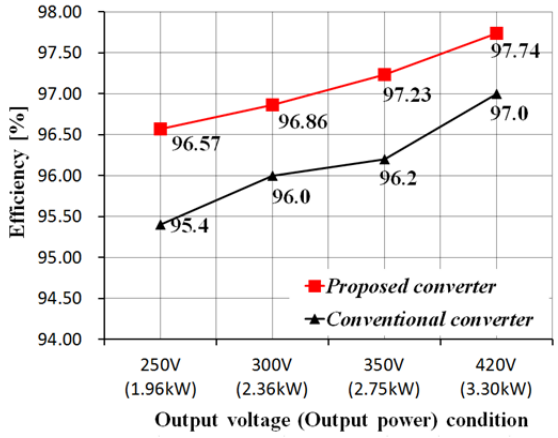

(a)

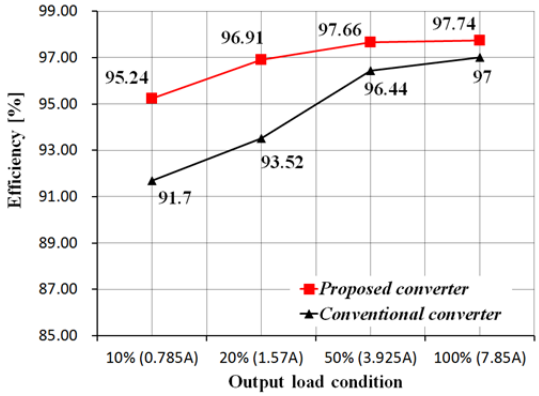

(b)

Fig. 12 Efficiency measured with the battery charging profile with constant-current mode and constant-voltage mode: (a) Efficiency during constant-current mode with the charging current of 7.85A and (b) efficiency during constant-voltage mode at 420V.

charging process. As shown in Fig. 12, the proposed converter has better performance than the conventional PSFB converter. This is due to the reduced circulating current, wider ZVS range, ZCS operation of all of the rectifier diodes, and lower turns-ratio. The proposed converter has a maximum efficiency of 97.74% under the full load condition and it maintains high efficiency during the battery charging process.

IV. CONCLUSION

In order to improve the performance of the conventional PSFB converter for EV battery charger applications, hybrid type converters have been recently researched. In this paper, a new hybrid DC-DC converter with a full-bridge rectifier has been presented. While the proposed converter has all of the benefit mentioned for the hybrid converters in [12]-[14], the proposed converter has fewer components and better utilization of the transformers when compared with the previously presented hybrid converters. A summary of the advantages is given as follows:

1) Full ZVS range of all of the active switches without a d uty-cycle loss
2) ZCS turn-off operation of the rectifier diodes
3) Minimized circulating current
4) Smaller output filter inductor
5) Better utilization of the transformers for battery charger applications

Experimental results with a 3.3 kW prototype converter show a 97.74% peak efficiency and a high efficiency during the battery charging process. From these results, it can be said that the proposed converter is suitable for EV battery on-board charger applications.

REFERENCES

[1] M. Pahlevaninezhad, P. Das, J. Drobnik, G. Moschopoulos, P. Jain, and A. Bakhshai, "A nonlinear optimal control approach based on the control-lyapunov function for an AC/DC converter used in electric vehicles," *IEEE Trans. Ind. Informatics*, Vol. 8, No. 3, pp. 596-612, Mar. 2012.

[2] B.-Y. Chen and Y.-S. Lai, "New digital-controlled technique for battery charger with constant current and voltage control without current feedback," *IEEE Trans. Ind. Electron.*, Vol. 59, No. 3, pp. 1545-1553, Mar. 2012.

[3] C. Nguyen and H. Lee, "Robust and unity input power factor control scheme for electric vehicle battery charger," *Transactions of Korean Institute of Power Electronics(KIPE)*, Vol. 20, No. 2, pp. 182-192, Apr. 2015.

[4] M. Yilmaz and P. T. Krein, "Review of battery charger topologies, charging power levels, and infrastructure for plug-in electric and hybrid vehicles," *IEEE Trans. Power Electron.*, Vol. 28, No. 5, pp. 2151-2169, May 2013.

[5] S. Jung, S. Hong, J. Park, and S. Choi, "A 3.3kW Bi-directional EV charger with V2G and V2H function," *Transactions of Korean Institute of Power Electronics(KIPE)*, Vol. 20, No. 1, pp. 31-37, Feb. 2015.

[6] B. P. McGrath, D. G. Holmes, P. J. McGoldrick, and A. D. McIver, "Design of a Soft-Switched 6-kW Battery Charger for Traction Applications," *IEEE Trans. Power Electron.*, Vol. 22, No.4, pp. 1136-1144, Jul. 2007.

[7] D. Gautam, F. Musavi, M. Edington, W. Eberle, and W. G. Dunford, "An automotive on-board 3.3kW battery charger for PHEV application," *IEEE Trans. Veh. Technol.*, Vol. 61, No. 8, pp. 3466-3474, Oct. 2012.

[8] B. Whitaker, A. Barkley, Z. Cole, B. Passmore, D. Martin, T. R. McNutt, A. B. Lostetter, J. S. Lee, and K. Shiozaki, "A high-density, high-efficiency, isolated on-board vehicle battery charger utilizing silicon carbide power devices," *IEEE Trans. Power Electron.*, Vol. 29, No. 5, pp. 2606-2617, May 2014.

[9] I. Lee and G. Moon, "Phase-shifted PWM converter with a wide ZVS range and reduced circulating current," *IEEE Trans. Power Electron.*, Vol. 28, No. 2, pp. 908-919, Feb. 2013.

[10] I. Lee and G. Moon, "Soft-switching DC/DC converter with a full ZVS range and reduced output filter for high-voltage applications," *IEEE Trans. Power Electron.*, Vol. 28, No.1, pp. 112-122, Jan. 2013.

[11] I. Lee and G. Moon, "Analysis and design of phase-shifted dual H-bridge converter with a wide zvs range and reduced

output filter," *IEEE Trans. Ind. Electron.,* Vol. 60, No.10, pp. 4415-4426, Oct. 2013.
[12] W. Yu, J. Lai, W. Lai, and H. Wan, "Hybrid resonant and PWM converter with high efficiency and full soft-switching range," *IEEE Trans. Power Electron.,* Vol. 27, No. 12, pp. 4925-4933, Dec. 2012.
[13] C. Liu, B. Gu, J. Lai, M. Wang, Y. Ji, G. Cai, Z. Zhao, C. Chen, C. Zheng, and P. Sun, "High-efficiency hybrid full-bridge-half-bridge converter with shared lagging-leg and dual outputs in series," *IEEE Trans. Power Electron.,* Vol. 28, No.2, pp.849-861, Feb. 2013.
[14] B. Gu, C. Lin, B. Chen, J. Dominic, and J. Lai, "Zero-voltage-switching PWM resonant full-bridge converter with minimized circulating losses and minimal voltage stresses of bridge rectifiers for electric vehicle battery chargers, " *IEEE Trans. Power Electron.,* Vol. 28, No. 10, pp. 4657-4667, Oct. 2013.
[15] I. Lee and G. Moon, "Half-bridge integrated ZVS full-bridge converter with reduced conduction loss for electric vehicle battery chargers," *IEEE Trans. Ind. Electron.,* Vol. 61, No. 8, pp. 3978-3988, Aug. 2014.

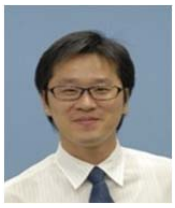

Il-Oun Lee received his B.S degree in Electrical and Electronic Engineering from Kyungpook National University, Taegu, Korea, in 2000; his M.S. degree in Electrical Engineering from Seoul National University, Seoul, Korea, in 2002; and his Ph.D. degree from the Korea Advanced Institute of Science and Technology (KAIST), Daejeon, Korea, in 2013. From 2003 to 2008, he was a R&D Engineer in the PDP (Plasma Display Panel) Development Group, Samsung SDI, Korea, where he was involved in circuit and product development. From 2008 to 2013, he was a Senior Engineer in the Power Advanced Development Group, Samsung Electro-Mechanics Co. LTD., Korea, where he was involved in the development of EV battery chargers, LED lighting drivers, high efficiency server or network power supplies, and high power density adapters. From 2013 to 2015, he was a Senior Researcher in the Energy Saving Lab., Korea Institute of Energy Research (KIER), Daejeon, Korea, where he carried out research on advanced high reliability microgrids and the development of a simulator system for a 20kW diesel engine generator. In 2015, he joined the School of Electrical and Electronic Engineering, Keimyung University, Daegu, Korea, as an Associate Professor. His current research interests include DC-DC converters, power factor correction (PFC) AC-DC converters, LED drivers, battery chargers for electric vehicles, digital display power systems, and digital control approaches for DC-DC converters.